Negative Magnetic Permeability in the Visible Light Region

Atsushi Ishikawa,[1,2] Takuo Tanaka,[1,*] and Satoshi Kawata[1,2]

[1]*Nanophotonics Laboratory, RIKEN Hirosawa, Wako, Saitama 351-0198, Japan*
[2]*Department of Applied Physics, Osaka University Yamadaoka, Suita, Osaka 565-0871, Japan*

Negative magnetic permeability of single split-ring resonators (SSRRs) is theoretically investigated in the visible light region. To describe the conduction characteristics of metal in the visible range, we develop the internal impedance formula completely. In our calculations, we determine the magnetic responses of the SSRR accurately. Based on our investigations, we also demonstrate the negative μ of the silver SSRR array in the visible light region.

Recently, controlling optical properties of materials by an array of metallic subwavelength-structured objects has attracted much interest from researchers. This artificial material referred to as ''metamaterial'' conceptually enables us to freely specify the permittivity (ε) and the permeability (μ) in a particular frequency region. In particular, a split-ring resonator (SRR) [1], which acts as an artificial magnetic atom, is a powerful tool for obtaining a negative μ, with which we can create a left-handed material (LHM) exhibiting unique electromagnetic phenomena [2]. By using the SRR, negative μ materials and LHMs have already been demonstrated in the microwave region [3,4].

On the other hand, in the high frequency region above THz, it was believed that obtaining strong magnetic responses from such metallic structures is impossible because of Ohmic loss. However, recently some experimental studies on magnetic properties of SRRs have been reported at 1 THz [5], at 60 THz [6], and particularly at 100 THz [7], and now the interest of this field is moving to the visible light range. As a result, further investigations regarding the SRR's properties in the visible range are eagerly anticipated, and they could open new possibilities for realizing negative μ materials or LHMs in the visible light region.

In this Letter, we investigate theoretically the magnetic responses of the single SRRs (SSRRs) in the visible light region. The primary difference between this study and the previous investigation [8,9] is that the complete formula of the internal impedance, which is valid throughout the frequency range, is used to describe the metal's properties.

In the optical frequency region, the conductivity of a metal is described as

$$\sigma(\omega) = \frac{\omega_p^2 \varepsilon_0}{\gamma - i\omega}, \qquad (1)$$

where ω_p is the plasma frequency and γ is the damping constant of the material. By using Eq. (1), in the previous study, the internal impedance for a unit length and a unit width of a plane conductor $Z_s(\omega)$ was defined as

$$Z_s(\omega) = \frac{1}{\sigma(\omega)\delta(\omega)} = R_s(\omega) + iX_s(\omega), \qquad (2)$$

where $\delta(\omega)$ is the skin depth [10]. The real and imaginary parts of $Z_s(\omega)$ are the surface resistivity R_s and the internal reactance X_s, respectively. In the optical frequency region, Eq. (2), including the skin effect, enables us to describe the conduction characteristics properly. However, particularly in the frequency region above 100 THz, which is our interest, we must consider not only the delay of the current but also the displacement current inside the metal. To describe these phenomena, we derived the following equation for the internal impedance of the plane conductor from the Maxwell's equations without any approximation:

$$Z_s'(\omega) = \sqrt{\frac{\mu_0}{\varepsilon_0(1 + i\frac{\sigma(\omega)}{\varepsilon_0\omega})}} = R_s'(\omega) + iX_s'(\omega), \qquad (3)$$

where ε_0 and μ_0 are the permittivity and the permeability of vacuum, respectively. Note that the ''1'' in the denominator of Eq. (3) represents the effect of the displacement current inside the metal as opposed to that of the conduction current, and this term describes the dielectric-like behavior of the metal in the visible range.

Figure 1 shows the dispersion curves of the surface resistivity R_s and the internal reactance X_s of silver, gold, and copper calculated by using Eq. (2) (the curves labeled a and c) and Eq. (3) (the curves labeled b and d). In our calculations, we used the empirical values $\omega_p = 14.0 \times 10^{15}$ s^{-1} and $\gamma = 32.3 \times 10^{12}$ s^{-1} for silver, $\omega_p = 13.8 \times 10^{15}$ s^{-1} and $\gamma = 107.5 \times 10^{12}$ s^{-1} for gold, and $\omega_p = 13.4 \times 10^{15}$ s^{-1} and $\gamma = 144.9 \times 10^{12}$ s^{-1} for copper [11]. There are notable differences of the R_s variations between curves a and b, suggesting that Eq. (2) fails both qualitatively and quantitatively in the visible light region. In contrast with the curves a, which keep increasing, the curves b saturate at the inherent frequency of each metal after first increase. In addition, Eq. (3) describes another increase of R_s in the visible range, which is the dielectric-like behavior of the metal. On the other hand, there is really not much difference of the X_s variations between curves c
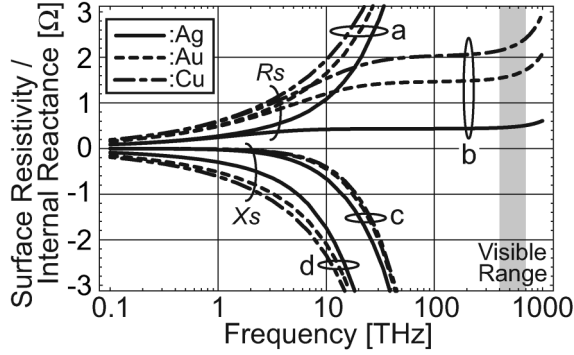
FIG. 1.   Dispersion curves of the internal impedance of silver, gold, and copper; the curves labeled a and b are the surface resistivity R_s calculated by using Eqs. (2) and (3), respectively; the curves labeled c and d are the internal reactance X_s calculated by using Eqs. (2) and (3) respectively.

and d, and they have a large negative value as the frequency increases. As a result, in the visible range, we must pay attention to the effect of the large negative X_s on the SRR's behavior rather than that of R_s, which is expected to be constant.

By using Eq. (3), we investigated the magnetic responses of the metallic SSRRs in the visible light region. At frequencies above 100 THz, the SRR consisting of a single ring, as shown in Fig. 2, is appropriate because the small geometrical capacitance of the SSRR realizes a high resonant frequency effectively [8]. Figures 2(a) and 2(b) depict our calculation model of the SSRR structure and the array of the SSRRs placed in a host material whose relative permittivity is ε_r. The SSRR consists of a single ring with N divisions around the ring, and we set $N = 2$ in our calculations. For simplification, we considered the ring thickness to be the same as the penetration depth $\tau(\omega)$, which is given by

$$\tau(\omega) = \mathrm{Re}\left[\frac{\delta(\omega)}{1 - i}\right]. \qquad (4)$$

In the visible range, the decrease of the penetration depth $\tau(\omega)$ is already saturated approximately at 20 nm.
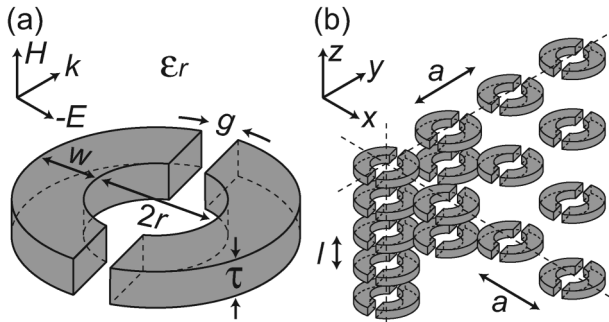

FIG. 2.   Models of SSRR used in our calculations. (a) The element of the SSRR, and (b) the array of the SSRR placed in the host material whose relative permittivity is ε_r.

The basic form of the effective permeability of the SRRs is derived from Refs. [8,9] and given by

$$\mu_{\mathrm{eff}} = \mu_{\mathrm{Re}} + i\mu_{\mathrm{Im}} = 1 - \frac{F\omega^2}{\omega^2 - \frac{1}{CL} + i\frac{Z(\omega)\omega}{L}}, \qquad (5)$$

where F is the filling factor, ω is the angular frequency, C and L are the geometrical capacitance and inductance, and $Z(\omega)$ is the ring metal impedance. In the case of our calculation model, F, C, L, and $Z(\omega)$ are represented by

$$F = \frac{\pi r^2}{a^2}, \qquad (6)$$

$$C = \frac{1}{N}\varepsilon_0\varepsilon_r\frac{w\tau(\omega)}{g}, \qquad (7)$$

$$L = \frac{\mu_0\pi r^2}{l}, \qquad (8)$$

and

$$Z(\omega) = \frac{2\pi r Z_s'(\omega)}{w}, \qquad (9)$$

where r is the radius of the ring, w is the width of the ring, g is the gap distance of the division, a is the unit-cell dimension in the xy plane, and l is the distance between adjacent planes of the SRRs along the z axis.

Figure 3 shows the relationship between both the real and imaginary parts of the effective permeability (μ_{Re}, μ_{Im}) of the silver SSRRs and the dimensions of the SSRRs. In our calculations, g and l were kept constant, which leads to practical scaling of the SSRR, and we set $\varepsilon_r = 2.25$ (e.g., glass). As the dimensions of the SSRRs decrease, the magnetic response, which is defined by the
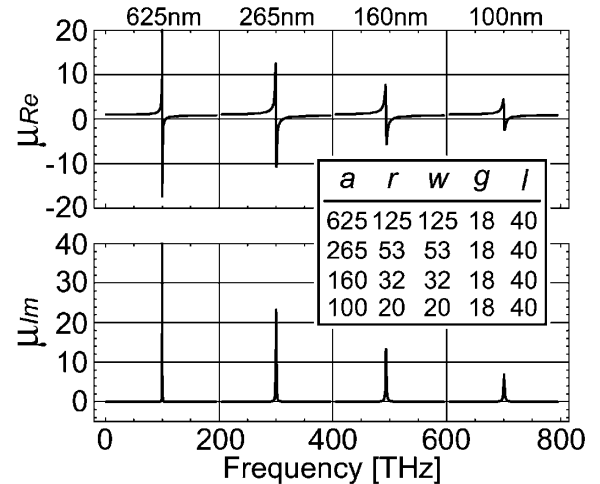

FIG. 3.   Real and imaginary parts of the effective permeability of the silver SSRRs in the host material ($\varepsilon_r = 2.25$) as a function of the SSRRs' dimensions. The labeling in each case indicates the unit-cell dimension a. The inset shows the corresponding dimensions of the SSRR in nanometers.

difference between maximum μ_{Re} and minimum μ_{Re}, decreases. At the same time, the resonant frequency shifts to a high value. Note that the calculated resonant frequency does not satisfy the scaling law because of the large negative X_s, as shown in Fig. 1

In order to understand the SSRRs' behavior in the visible light region, we calculated the frequency dependencies of the minimum μ_{Re} under the same calculation condition. Figure 4 shows the calculation results for the SSRRs made of silver, gold, and copper, respectively. In Fig. 4, the μ_{Re} minimum frequency dependence of the unit-cell dimension a of the silver SSRRs is also shown. As the frequency increases, the minimum μ_{Re} approaches unity asymptotically. The silver SSRRs still exhibits enough negative μ_{Re} throughout the visible range, as compared to the SSRRs made of gold and copper. The differences among these magnetic responses can be described by the differences of R_s, as shown in Fig. 1. In contrast with the R_s of gold and copper, which begin to drastically increase again from about 200 THz, that of silver is still constant throughout the visible range, suggesting that the resistance in the silver ring is also constant. As a result, we concluded that in the visible light region, the resistance in the ring is not a dominant factor for the silver SSRRs to realize the negative μ.

In order to describe the SSRRs' behavior in terms of the filling factor F, we calculated the minimum μ_{Re} of the SSRRs made of silver, gold, and copper by changing F. Figures 5(a)–5(c) show the calculation results for the SSRRs made of silver, gold, and copper, respectively. The frequency dependencies of the imaginary part of the effective permeability whose real part has the minimum value are also shown. As shown in Fig. 5(a), the silver SSRRs has a large tunable range of μ_{Re} by changing F, and it exhibits a negative μ_{Re} throughout the visible range with just a small $F = 5\%$ ($a = 158.5$ nm). On the other hand, in the case of gold and copper, the tunable range of μ_{Re} is small; therefore, a high F, which results in a high-

scattering loss, is necessary to realize a usable negative μ_{Re} in the visible range. From Fig. 5, we also calculated the $|\mu_{Im}|/|\mu_{Re}|$ ratio proposed by Dimmock to estimate the absorption loss [12], and we obtained 1.146, 1.787, and 2.788, all with $F = 11\%$ at 400 THz for the SSRRs made of silver, gold, and copper, respectively. These calculation results also predict that silver is the most appropriate metal to realize a practical negative μ material in the visible light region.

In conclusion, we investigated the negative μ of the SSRRs in the visible light region. In our theoretical analysis, we considered the effect of the displacement current, which was shown to determine the SSRR's behavior in the visible range. Our results indicate that the resistance in the ring is not a dominant factor for the negative μ of the silver SSRRs because R_s of silver is constant in the visible range.

FIG. 5. Frequency dependencies of the minimum μ_{Re} of the SSRRs made of (a) silver, (b) gold, and (c) copper according to the filling factor: $F = 3\%$, 5%, 7%, 9%, and 11%. The μ_{Re} minimum frequency dependencies of μ_{Im} are also shown.
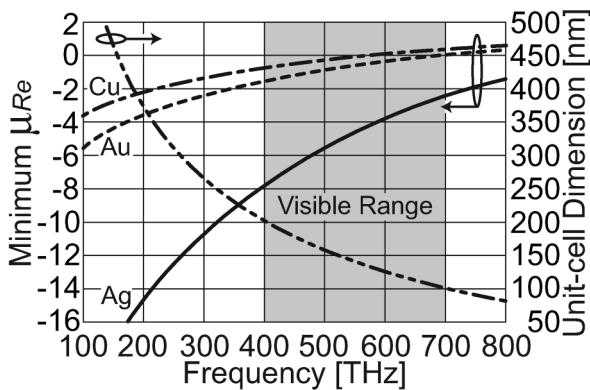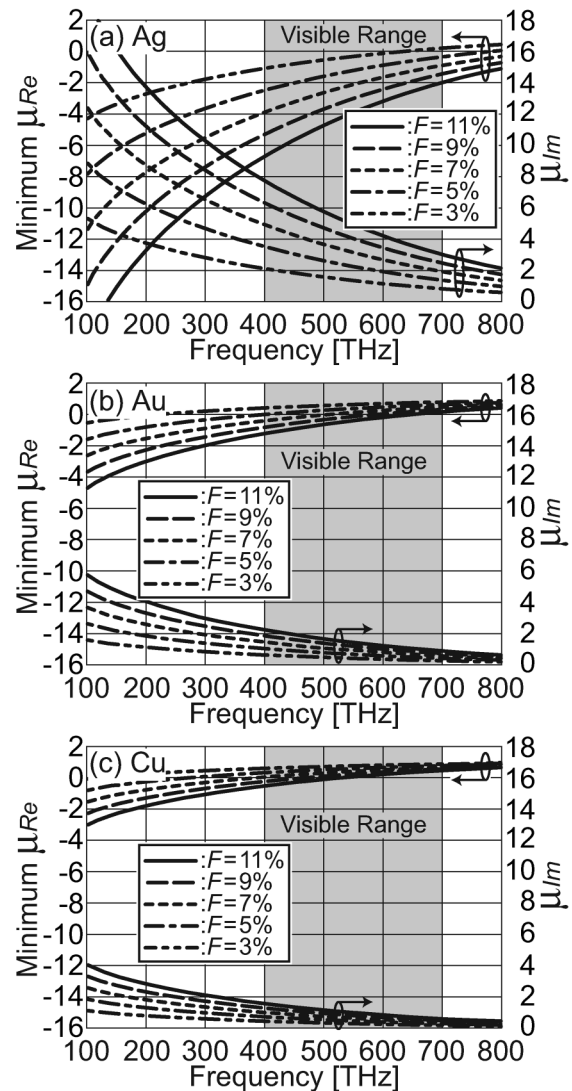

FIG. 4. Frequency dependencies of the minimum μ_{Re} of the SSRRs made of silver, gold, and copper. The μ_{Re} minimum frequency dependence of the unit-cell dimension a of the silver SSRRs is also shown.

We also claim, based on our investigations, that the silver SSRR array realizes the negative μ in the visible light region. Recently, Shalaev and his colleagues proposed a simple structure consisting of a parallel nanorod array for both the negative μ and ε in the optical frequency region [13]. This structure is also a suitable candidate for a practical negative μ material or LHM in the visible light region. In addition, when the size of the SSRR structure becomes excessively small ($\sim$nm), we must consider an additional dissipation resulting from surface plasmon excitation and Landau damping in the nanogap, as predicted by Larkin *et al.* [14]. In this Letter, we used a large enough gap to minimize these effects.

---

*Corresponding author.
Email address: t-tanaka@riken.jp

[1] J. B. Pendry, A. J. Holden, D. J. Robbins, and W. J. Stewart, IEEE Trans. Microwave Theory Tech. **47**, 2075 (1999).

[2] V. G. Veselago, Sov. Phys. Usp. **10**, 509 (1968).

[3] D. R. Smith, W. J. Padilla, D. C. Vier, S. C. Nemat-Nasser, and S. Schultz, Phys. Rev. Lett. **84**, 4184 (2000).

[4] R. A. Shelby, D. R. Smith, and S. Shultz, Science **292**, 77 (2001).

[5] T. J. Yen, W. J. Padilla, N. Fang, D. C. Vier, D. R. Smith, J. B. Pendry, D. N. Basov, and X. Zhang, Science **303**, 1494 (2004).

[6] S. Zhang, W. Fan, B. K. Minhas, A. Frauenglass, K. J. Malloy, and S. R. J. Brueck, Phys. Rev. Lett. **94**, 037402 (2005).

[7] S. Linden, C. Enkrich, M. Wegener, J. Zhou, T. Koschny, and C. M. Soukoulis, Science **306**, 1351 (2004).

[8] S. O'Brien and J. B. Pendry, J. Phys. Condens. Matter **14**, 4035 (2002).

[9] S. O'Brien, D. McPeake, S. A. Ramakrishna, and J. B. Pendry, Phys. Rev. B **69**, 241101 (2004).

[10] The expression of Eq. (2) is unspecified in Ref. [8], but it can be obtained from Eqs. (12)–(15) in Ref. [8] by simple mathematical procedures.

[11] P. B. Johnson and R. W. Christy, Phys. Rev. B **6**, 4370 (1972).

[12] J. O. Dimmock, Opt. Express **11**, 2397 (2003).

[13] V. A. Podolskiy, A. K. Sarychev, and V. M. Shalaev, Opt. Express **11**, 735 (2003).

[14] I. A. Larkin, M. I. Stockman, M. Achermann, and V. I. Klimov, Phys. Rev. B **69**, 121403 (2004).